Spring 2023

Hydrological patterns of the Chimborazo Reserve: Streamflow, climate, and glacier recession data show a loss of glacial influence on the southwestern aspect of the Chimborazo volcano, Ecuador.

William F. M. Patrick
SIT Study Abroad

Hydrological patterns of the Chimborazo Reserve

Streamflow, climate, and glacier recession data show a loss of glacial influence on the southwestern aspect of the Chimborazo volcano, Ecuador.

School for International Training, 1 Kipling Road, Brattleboro, VT 05301

William F. M. Patrick

Academic Director: Dr. Xavier Silva, Ph.D.
Project Advisor: Ana María Ortega, M.S.

Pomona College
Environmental Biology

Canton Riobamba, Chimborazo Province, Ecuador

Submitted in partial fulfillment of the requirements for Ecuador: Comparative Ecology & Conservation, SIT Study Abroad, Spring 2023

ABSTRACT

The Chimborazo volcano of the central Ecuadorian Andean Cordillera (6310 m) has been shown to currently be undergoing extreme glacial recession due to climate change. For this reason, this study sought to analyze climate and glacier recession data in conjunction with streamflow from kryal (glacial-fed), rhithral (non-glacial-fed), and intermediate streams to not only evaluate the current health of Chimborazo's glaciers, but also determine how hydrology in the region will respond to future climate change. The rate of glacial recession on the volcano was determined using satellite imagery between 1965 and 2019. Measurements of stream elevation, pH, water temperature, width, depth, and turbidity were taken at a total of 11 sites, 4 kryal sites, 4 rhithral sites, and 3 intermediate sites. Climate data was measured over the course of 20 days and used in comparison with stream data. An estimation of overall glacial recession of 42.5% was made between 1965 and 2019, with this value most likely being higher on the southwestern aspect of the volcano where data was collected. Kryal streams were observed to encompass the greatest range of water temperature in any stream-type, with their coldest temperatures between 5.5 and 7.5 ˚C already being too warm for the upper limits of kryal streams. Rhithral streams generally responded to differences in precipitation and air temperature more than kryal streams. However, the kryal stream with a source deeper in the volcano's rain shadow responded similarly to rhithral streams. Together, these data implied a lower degree of glacial influence, with the least influence farthest into Chimborazo's rain shadow. Furthermore, it exemplified that there no longer exist truly kryal streams on the volcano's southwestern aspect. Implications of this data include that streams in this part of the reserve will become more susceptible to climate change in the future, as glacial influence all but disappears.

RESUMEN

Se ha demostrado que el volcán Chimborazo de la Cordillera de los Andes ecuatorianos centrales (6310 m) actualmente está experimentando una recesión glacial extrema debido al cambio climático. Por esta razón, este estudio procuró analizar los datos de clima y de recesión glaciar en conjunto con el flujo de corrientes kryales (alimentados por glaciares), ritrales (alimentados por no glaciares) y intermedias con el fin de no solo evaluar la salud actual de los glaciares de Chimborazo, sino también determinar cómo la hidrología en la región reaccionará ante el cambio climático en el futuro. La tasa de recesión glacial en el volcán fue determinada usando imágenes satelitales entre 1965 y 2019. Medidas de la altura pH, temperatura del agua, ancho, profundidad, y turbidez de las corrientes se tomaron en un total de 11 sitios, 4 sitios kryales, 4 sitios ritrales y 3 sitios intermedios. Datos climáticos se midieron en el transcurso de 20 días y se utilizaron en comparación con los datos de flujo. Se realizó una estimación de la recesión glacial total del 42,5% entre 1965 y 2019, siendo este valor más alto en el aspecto suroeste del volcán donde se recolectaron los datos.Se observó que los riachuelos kryales abarcaban el mayor rango de temperatura del agua en cualquier tipo de riachuelo, con sus temperaturas más frías entre 5,5 y 7,5 ℃ siendo ya demasiado cálidas para los límites superiores de los riachuelos kryales verdaderos. Los riachuelos ritrales generalmente respondieron a las diferencias de precipitación y temperatura del aire más que los kryales. Sin embargo, el riachuelo kryal con una fuente más profunda en la sombra de lluvia del volcán volvió a responder de manera similar a los riachuelos ritrales. En conjunto, estos datos demostraron un bajo grado de influencia glacial, con la menor influencia en la sombra de lluvia de Chimborazo. Además, ejemplificaron que ya no existen verdaderos riachuelos kryales en el aspecto suroeste del volcán. Las implicaciones de estos datos incluyen que los riachuelos en esta parte de la reserva serán más susceptibles al cambio climático en el futuro, a medida que la influencia glacial casi desaparezca.

ACKNOWLEDGMENTS

I would like to first and foremost thank Ana María Ortega, M.S. for her help in the development of methodology, interpretation of data, and writing process of this study. Her help was instrumental, and this study would not be possible without it. I would also like to thank program directors Dr. Xavier Silva, Ph.D. and Diana Serrano, M.S. for their help in the formulation of this project, as this study would not exist without their input. I would also like to thank the Pulinguí San Pablo community at large, especially Manuel, for their kindness and hospitality during the month spent in the Chimborazo Reserve. As an extension of this, I would like to thank Anita, Fausto, and Benjamin for providing a welcoming environment in Casa Cóndor throughout the study period and would like to thank our primary contact at Casa Cóndor, Miguel Guamán, for his help in answering any questions we had, transporting us to Riobamba to buy groceries, and showing us the locations of data collection sites. His knowledge of the region was critical in the success of this study. Words cannot express how grateful I am to everyone who made this project a reality. Thank you all so much!

AGRADECIMIENTOS

En primer lugar, quiero agradecer a Ana María Ortega, M.S., su ayuda en el desarrollo de la metodología, la interpretación de los datos y el proceso de redacción de este estudio. Su ayuda fue instrumental, y este estudio no sería posible sin ella. También quiero agradecer a los directores del programa, Dr. Xavier Silva, Ph.D. y Diana Serrano, M.S. por su ayuda en la formulación de este proyecto, ya que este estudio no existiría sin su aporte. También me gustaría agradecer a la comunidad de Pulinguí San Pablo en general, especialmente Manuel, por su amabilidad y hospitalidad durante el mes pasado en la Reserva Chimborazo. Como una extensión de esto, me gustaría dar las gracias a Anita, Fausto, y Benjamin por crear un ambiente acogedor en Casa Cóndor durante todo el período de estudio, y a nuestro contacto principal en Casa Cóndor, Miguel Guamán, por su ayuda en responder a cualquier pregunta que tuviéramos, transportarnos a Riobamba para comprar comestibles, y mostrarnos las ubicaciones de los sitios de recopilación de datos. Su conocimiento de la región fue fundamental para el éxito de este estudio. Las palabras no pueden expresar lo agradecido que estoy a todos los que hicieron una realidad este proyecto. ¡Muchas gracias a todos!

INTRODUCTION

The Chimborazo-Carihuairazo massif of central Ecuador constitutes one of the largest glacier-capped volcanic systems in the northern Andes mountains, as well as the country's highest elevation region, reaching a maximum of 6,310 m (Clapperton, 1990). The area surrounding the massif below 5,000 m consists of páramo, an alpine habitat of generally cold and humid climate that exists above the tree line in the Northern Andes. At greater than 5,000 m of elevation, the mountainside gives way to rock, snow, and ice.

Given Chimborazo's high elevation, it serves as an obstruction to northeasterly trade winds, causing the mountain to have shifted gradients of humidity with more humid areas found on its northeastern face. The superpáramo belt, the transition line between permanent snow coverage and classical páramo ecosystem, is thus at a lower elevation on the windward side of the mountain (Sklenář and Lægaard, 2003). Additionally, these shifted gradients of humidity have created a rain shadow and subsequent desert on the volcano's southwestern aspect (**Figure 1.1**), a phenomenon unique to Chimborazo alone (Sklenář and Lægaard, 2003). These climatic differences have yielded a discrepancy in glacier thickness and elevation between east and west sides of the mountain over time, with glaciers of the eastern slopes growing thicker and extending 500 m lower than those of the western slopes (Sklenář and Lægaard, 2003).

Figure 1.1. Arenal Grande arid paramo zone on the Chimborazo volcano's southwestern aspect.

A current body of research suggests that while Chimborazo's glaciers experienced natural expansions and contractions in the last 50,000 years (Clapperton, 1990), the melting of glaciers on the volcano in the present day is most likely due to anthropogenic climate change (Alvarez-Mendoza and Ramirez-Cando, 2022). Current instrumental records have indicated a local warming at the massif of about 0.10 ˚C per decade in the last 70 years (Rabatel et al., 2013). In roughly the same period, the glaciers on the Chimborazo volcano lost 21% (± 9%) of their ice-covered surface area (La Frenierre and Mark, 2017). This trend, although already a negative one, is even more worrisome when compared to glacier reduction data from around the world, as the mean balance deficit of glaciers in the Andes is on average slightly more negative than those of the rest of the globe (Rabatel et al., 2013). This trend in glacier shrinkage in the tropical Andes may be explained through the combination of an increase in the frequency of El Niño events since the late 1970s, as well as a general warming of the troposphere due to CO2 emissions (Rabatel et al., 2013).

Despite these changes in atmospheric temperature and weather patterns, studies have maintained that precipitation affecting the Chimborazo-Carihuairazo massif has remained largely unchanged (La Frenierre and Mark, 2017). Residents of the Chimborazo area, however, especially on the volcano's southwestern face within its rain shadow, have reported a noticeable reduction in rainfall and surface water availability in the last few decades. The near unanimity of these observations in contrast with the scientific literature suggests that this result has not yet appeared in the metrics used in these studies (La Frenierre and Mark, 2017).

Studies published in various scientific journals have also found that there is a strong correlation between higher elevation ecosystems and a larger degree of temperature increase due to climate change (Sklenář et al., 2021; Mountain Research Initiative Edw Working Group et al., 2015; Aguilar-Lome et al., 2019; Rangwala and Miller, 2012). This larger degree of temperature change has yielded more liquid precipitation over glaciers. This is especially notable on Chinborazo's southwestern aspect, where it causes greater melting of glaciers and further lack of solid precipitation to replenish lost ice (Gordillo and Pineda, 2021). Thus, Chimborazo's high altitude must play a critical role in its changing environment.

One method for measuring glacial health involves streamflow. There are three accepted types of high elevation runoff that are found in alpine regions globally. *Kryal* streams are those fed by glacial meltwater and are generally of a very low temperature (maximum 4 ˚C). They generally lack vegetation cover due to being located at higher altitude and in more windswept regions. This lack of vegetation generally leads these streams to have greater temperature increases, albeit to temperatures that are not very warm (Trimmel et al., 2018). *Rhithral* streams are those consisting of runoff from rainfall and extended periods of snowmelt, usually encompassing a wider range of temperatures than that of kryal streams. These streams are generally surrounded by farmland because of lower elevation, and organic matter left behind by domesticated animals in these areas raises water pH (Irshad et al., 2013). Finally, *krenal* streams are those fed by groundwater, contain relatively high concentrations of calcium carbonate and constant flow regimes (Steffan, 1971; Ward, 1994). The water temperature of these streams generally is equal to the mean annual air temperature above ground, and shows little variation (Kaandorp et al., 2019). These stream types are found in equatorial alpine regions as well as in temperate ones, albeit at higher elevations due to higher air temperatures credited to greater sunlight intensity (Jacobsen et al., 2009).

Glaciers are related to streamflow in several ways. First, in equatorial regions such as the Andes, glacier coverage is the most important factor for streamflow and temperature regulation in kryal streams (Stahl et al., 2008; Williamson et al., 2019). First, it is generally accepted that kryal streams on the equator show less variation in flow yearly and more variation daily. This is due to the distinct lack of freezing and thawing seasons in tropical alpine regions. There is never a time during the year when a stream is not flowing; instead, in tropical alpine regions, the intensity of the sun during daylight hours begins the melting process on glaciers, and streamflow increases. Conversely, during the night, melting virtually stops, and stream flow is decreased by morning (Jacobsen et al., 2009). Second, glaciers on the equator are known to regulate streamflow and water temperature during wet and dry periods. During drier periods, glacial melt increases due to lack of solid precipitation, both increasing streamflow and compensating for warmer air temperatures by cooling base water temperature; the opposite occurs during wetter periods, with glacial melt being replenished, decreasing streamflow and compensating for cooler air temperatures by increasing base water temperature (Stahl et al., 2008).

As glaciers continue to melt, however, streamflow will increase until an absolute maximum called ‘peak water’ is reached, where remaining glacial mass can no longer support increases in streamflow. From this point, streamflow will begin to decrease at significant rates, especially in the Andes, which are especially vulnerable due to their tropical location. As glaciers cross the ‘peak water’ threshold and become too small to regulate streamflow, they are overtaken in stream influence by air temperature and precipitation. A study conducted by Pellicciotti et al in 2007 showed streamflow in kryal streams of Andean catchments to correlate positively to phases of warmer weather. This phenomenon has begun to be observed in mountain ranges throughout the world, including the Andes (Huss and Hock, 2018; Marazi and Romshoo, 2018), where streams are now seeing not only increases in maximum flow but also decreases in minimum flow (Pabón-Caicedo et al., 2020; Ragettli et al., 2016) as they become more sensitive to the subtle wet and dry seasons. While overall stream output is unchanging, output during the wet season has begun to drastically increase, while that during the dry season has decreased to almost nothing (Pabón-Caicedo et al., 2020; Vuille, 2013; Pellicciotti et al., 2007). Streamflow in Northern Ecuadorian Andean basins on the southwestern aspects of mountains was recently shown by a study conducted by Gordillo and Pineda in 2021 to even respond to wet spells in the months of March, April, and May with increases in streamflow regimes. Compounded, these studies show that kryal streams are becoming more sensitive to minute changes in climate and are thus losing their distinct characteristics.

In short, as anthropogenic climate change progresses, weather will have a more significant effect on kryal streamflow than glacial melt itself (Pabón-Caicedo et al., 2020; Vuille, 2013). It is thus important to know whether glaciers on the

Chimborazo volcano have also already reached the ‘peak water’ threshold.

Given this past research, this study aims to determine the health of the glaciers on the Chimborazo southwestern aspect by analyzing differences in stream characteristics between rhithral, kryal, and intermediate streams, as well as determining to what extent these characteristics change with respect to weather throughout the study period.

The study seeks to answer this central question by 1) understanding water flow in a region where adequate research has not yet been conducted, and in one of those most being affected by climate change, and 2) studying how streams, rhithral, kryal and intermediate, respond to climate over the course of the month studied, thus gaining a better picture of how they will respond to climate change long-term.

This research into glacial recession and climate, and their effects on streamflow in the Chimborazo volcano region is crucial for understanding the health and sustainability of the páramo ecosystem. While a large amount of research has been done on the dynamics of climate, glacier reduction, and streamflow in alpine regions of temperate latitudes, particularly within the Northern hemisphere, far less has been done within the tropics (Rosenblüth et al., 1997). This research is crucial, as water bodies sourced in the páramo directly support the health of larger forest regions such as the Amazon, Choco, and wetland coastal areas by regulating the local climate, provide habitat for aquatic species, and support critical ecological processes such as nutrient cycling and sediment transport (Ely and Martin, 2018; Milner et al., 2017).

In addition, glaciers and water bodies in the páramo constitute vital sources of freshwater for domestic, agricultural, and industrial uses in Andean communities (Chevallier et al., 2010; Giles et al., 2018; Padrón et al., 2015; Milner et al., 2017).

Finally, this situation in Chimborazo is emblematic of wider changes occurring in the páramo regions of the Andes due to climate change. This is extremely important, as the central Andes account for 99% of the world’s tropical glaciers (Chevallier et al., 2010; Dyurgerov and Meier, 2005). Understanding what is occurring with glacier runoff stream quality and volume in Chimborazo will most likely be extrapolatable to other large mountains in the tropical Andes, including but not limited to Cayambe, Antisana, Cotopaxi, and others beyond Ecuador’s borders. By investigating the correlation between climate, glacial recession, and streamflow in the Chimborazo volcano region, this research has the potential to help inform the development of effective conservation and management strategies for the preservation of the Chimborazo Reserve, Northern Andean ecosystems at large, and ultimately, the health and well-being of the downstream ecosystems and human communities that depend on them.

MATERIALS, METHODS, & ETHICS

Stream and Site Selection

Water quality was measured at 5 different streams in a southern valley of the Chimborazo Reserve (**Figure 2.1**) near the Pulinguí San Pablo Community, 2 kryal on the northern wall of the valley, 1 intermediate within the valley itself, and 2 rhithral on the southern wall of the valley to serve as controls (**Figure 2.2**). Streams and measurement locations were previously determined through the work of Tanner Thomas in the months of April and May of 2022, and were used not only to gauge reliable locations for data collection but also to easily compare between his data and those of this experiment (Thomas, unpublished, 2022). Sites ranged in elevation between 3858 and 4175 m. Each stream was measured at 2 sites apart from the intermediate stream, which was measured at 3 sites. At each site, 3 places along a 10-meter section of stream were randomly selected and served as the locations of measurement for the duration of the study.

Stream Site Descriptions

Streams 1 and 2 were rhithral streams sourced on the elevated land to the south of the valley studied, with stream 1 feeding into stream 5 upstream of site 5a. Stream 1 was located in the southeast area of the valley. Site 1a was surrounded by semi-pasteurized land with compact soil and a lack of vegetation excluding cushion grass, while site 1b was located in a small ravine under a short waterfall with looser soil and ample vegetation (**Figure 2.2**, see Appendix B). Conversely, stream 2 was located in a deep ravine to the south. Site 2a was surrounded by alpaca-pasteurized land with ample vegetation and relatively loose soil, and it is important to note that the site had artificial qualities. Due to the presence of the Concreto Chimborazo company in lower elevation regions around the Pulinguí San Pablo community, streamflow at certain rhithral streams could be rechanneled to facilities (Concreto Chimborazo Worker, Personal Communication, 2023). Stream 2 was one such stream, and site 2a fell downstream of a rechanneling canal. Site 2b, however, was located upstream of this canal and was surrounded by non-pasteurized land with very loose soil. The site was located in a stream basin much wider than itself with very little vegetation, suggesting past exposure to flash-flooding (**Figure 2.2**, see Appendix B).

Streams 3 and 4 were kryal streams sourced on the slopes of the Chimborazo volcano to the north of the valley studied, with stream 4 feeding into stream 5 upstream of sites 5a and 5b. Stream 3 was located in the northeast of the valley. Sites 3a and 3b were both surrounded by non-pasteurized land with relatively compact soil and ample vegetation (**Figure 2.2,** see Appendix B). Conversely, stream 4 was located in the northwest corner of the valley. Site 4a was located in a large fluvial plain consisting of extremely loose soil surrounded by non-pasteurized land. The expanse of the fluvial plain with relation to the width of the stream at this site suggested past exposure to flash-flooding. Site 4b was located in a small ravine with ample vegetation consisting of relatively loose soil (**Figure 2.2**, see Appendix B).

Figure 2.1. Location of data collection site (A) within the country of Ecuador and (B) in relation to the Chimborazo volcano.

Stream 5 was an intermediate stream with both kryal and rhithral water located on the southern portion of the lowland area of the valley studied. Sites 5a, 5b, and 5c were surrounded by heavily pasteurized land with little vegetation excluding cushion and tussock grasses and consisted of generally compact soil. It is important to note that site 5c was located just downstream of a groundwater source (**Figure 2.2**, see Appendix B).

Figure 2.2. Data collection points in the Chimborazo Reserve. "a" points for each stream signify sites of lower elevation, while "b" points signify those of higher elevation.

List of Materials

Materials required for the experiment included a measuring pole, a Tactix 60-meter tape measure, a pH and temperature measurement device, plastic water collection jars, a stopwatch or similar mobile application, an altimeter or similar mobile application, the website Zoom Earth, and the desktop application Google Earth Pro.

Stream Characteristics and Qualities

While Thomas' experiment focused on the topic of macroinvertebrate biodiversity and its determination of water quality, this experiment focused on aspects of water quality alone, with the addition of climate and glacier recession data. Aspects of water quality and flow measured included pH, temperature, stream width, stream depth, stream velocity, altitude, and turbidity.

To understand how these data changed throughout the duration of the project, each site was measured a total of 4 times between the dates of April 18th and May 2nd, 2023. Additionally, to compare with climate data taken during the experiment and create a joint figure, the specific day of each data collection was denoted. Stream data collection was conducted in conjunction with a fellow student, Cole Pietsch, who was conducting further research on macroinvertebrate biodiversity and stream geomorphology in relation to stream health in the same area. Stream data was collected in tandem and at the same sites for collective data use upon analysis.

Stream Water Temperature and pH

Temperature and pH were collected together using an Apera Instruments pH20 pH Tester device. Data was collected in triplicate and averaged to yield more reliable values.

Stream Width

Stream width at each site was measured using a Tactix 60-meter tape measure at three aforementioned randomly selected sites along a 10-meter section of stream. In stream 5, waterflow sometimes extended below riverbank vegetation, and the tape measure was held underwater until a physical shore was reached. Values for stream width at each site were averaged in subsequent analysis. Stream width was used in data analysis only in calculating stream discharge.

Stream Depth

Stream depth at each site was measured using a bamboo pole and tape measure at the same three randomly selected sites as stream width. The pole was placed vertically into the stream until it struck the bottom, then removed with a placed finger to mark the water level. The distance from the tip of the bamboo pole to the finger was labeled stream depth. Values for stream depth at each site were averaged in subsequent analysis.

Stream depth was used in data analysis only in calculating stream discharge. Stream velocity was used in data analysis only in calculating stream discharge.

Stream Velocity

Stream velocity measurement at each site depended on the depth of the water present. If sufficiently deep, velocity was measured through the placement of a floating object tied to a string of known length (l) at a certain point on the stream (Chang, unpublished, 2019). Given that the string source was a certain height above the stream surface (h), the Pythagorean theorem was used to determine the distance that the object traveled at stream-surface level (d). The object was released, and the time in seconds taken for it to pull the string taut (t) recorded in triplicate. To determine velocity, the calculated stream-surface distance was divided by the time recorded (Chang, unpublished, 2019; Miranda, unpublished, 2019). If not sufficiently deep, stream velocity was measured via the placement of a tape measure of given length (d) alongside the stream, following its contours. A small object, usually a flower petal, was placed on the stream surface, and the time taken for the object to travel the given distance (t) was recorded in triplicate. To calculate velocity, the measured distance was divided by the time recorded. Velocity at each site was calculated using the average of triplicate time measurements to gain a more representative result (Thomas, unpublished, 2022).

$$stream\ velocity = \frac{d}{t} = \frac{\sqrt{l^2 + h^2}}{t}$$

Stream Discharge

Stream discharge was calculated in Microsoft Excel by multiplying the values of average stream width, average stream depth, and average stream velocity together. While this method is not perfect, it was determined sufficient, as it calculates the cross-sectional area of water in the stream moving per time if the stream were of a rectangular shape (**Figure 2.3**).

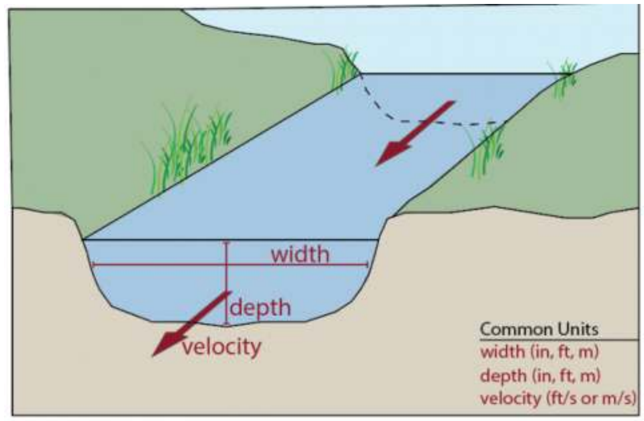

Figure 2.3. Visualization of crude calculation of stream discharge using stream width, stream depth, and stream velocity. Image: Andrew Wickert, GeomorphOnline.

Stream Turbidity

Turbidity at each site was measured through the collection of a water sample into a large plastic jar and its placement against a white background with black lines. The jar was shaken for 5 seconds, and an estimation from 0 to 5 was made using an index created for this study, with 0 being clear water with no particulate matter, and 5 being an inability to see the white background through the water.

Site Altitude

Altitude at each site was measured to the nearest 5 m using the mobile app AllTrails; this error margin was considered inconsequential given the degree of variation in altitude between stream sites.

Glacier Recession Data

Given that streamflow with relation to glaciers is the central theme of this project, past and current glacier data was searched for to relate these two variables together. Glacier recession data was taken using the desktop application Google Earth Pro, tracking glacier surface area coverage in the 54 years between 1965 and 2019. Surface area was estimated using the ‘polygon’ function in the application, tracing shapes around the glacier coverage in each image (**Figure 2.4**). Total surface area in km^2 was calculated by the application and recorded. Additional glacier surface area data in the years of 1986, 2000, and 2013 was pulled from a study about Chimborazo glacier recession (La Frenierre and Mark, 2017). All glacier recession data was plotted on the same axis to exemplify change over time.

Figure 2.4. Visualization of glacier surface area estimation using the 'polygon' feature of Google Earth Pro. The red line encircles one polygon measurement, while white lines around it show other measurements for reference.

Climate Data

In addition to streamflow and glacial recession data, this study incorporated climate data. The application Zoom Earth was used to collect climate data between April 15th and May 5th, 2023. After data collection, current data taken within the months of April and May 2023 was compared with data from the same months of the year 2022 in Thomas' study (Thomas, unpublished, 2022), allowing for a more complete analysis. Due to local observations of decreased precipitation in the area conflicting with scientific record, precipitation data was included in the study. Precipitation data was recorded in hourly values per day and summed to yield a total daily precipitation value. Actual air temperature data and relative humidity data were recorded in hourly intervals and averaged to gain average daily air temperature and relative humidity values.

Data Analysis

All data were analyzed using Microsoft Excel. Stream characteristic data was plotted on bar and whisker plots to show both value and range. Rates of change of stream pH, water temperature, and discharge rate with respect to elevation were also analyzed in bar plots. Finally, stream width was plotted against stream depth to discover any potential patterns.

Climate data was analyzed using scatterplots, including comparisons between total daily precipitation and both average daily relative humidity and average daily air temperature. This data was also plotted over time with respect to stream pH, water temperature, and discharge to discover any significant patterns. Stream discharge values were normalized using the first value calculated for each site to compare trends more easily over time in graphical form. Data for total daily precipitation and air temperature were each run through an unequal variance t-test with stream water temperature and discharge, and certain data was selected and subsequently elaborated on. Finally, all stream characteristics for rhithral, kryal, and intermediate streams were plotted on Principal Component Analyses (PCA) diagrams to discern overall correlations between variables. PCA helps to understand large data sets by reducing the number of variables in the set. By standardizing the ranges of the initial variables and selecting for a principal component that accounts for the largest possible variance, the other variables are ranked and compared to it. The reduced variables allow for machine learning algorithms to analyze the data points and makes it easier to explore and visualize the data. While the accuracy of relationships may be slightly reduced, he information is still contained and the understanding of relationships within it are simplified (Bro and Smilde, 2014).

Glacier recession data was analyzed using a scatter plot over time, and a trendline was created to discover its significance.

Study Precautions

To control for humidity and precipitation changes on different slopes of the Chimborazo volcano due to its rain shadow effect (Sklenář and Lægaard, 2003), all data was collected on its southwestern aspect. Additionally, due to the property of kryal streams at the equator to show variation in streamflow depending on time of day (Jacobsen et al., 2009), measurements at each specific site were conducted within a half hour of each other to account for this daily variation.

Ethical Considerations

First, the researchers acknowledge that this study was conducted on the ancestral lands of the Puruwá and Kichwa peoples. All data was collected using environmentally respectful and non-invasive procedures, although streambed sediment and vegetation surrounding sites were occasionally disrupted. Additionally, all data was collected on land owned by the Pulinguí San Pablo community. Impact on the community was minimized, and members of the community who aided in research were compensated. The study involved no human subjects, belonging to the community or otherwise.

RESULTS

Glacier Recession Data

The below trend ($R^2 = 0.85$) in Figure 3.1 shows Chimborazo glacial coverage decreasing by 42.5% from 20 km^2 in 1965 to 11.5 km^2 in 2019.

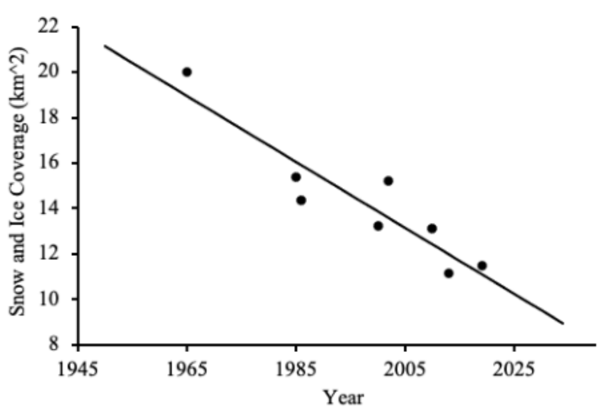

Figure 3.1. Chimborazo glacier surface area (km^2) between 1969 and 2019.

Stream Elevation

As depicted in Figure 4.1, elevation of sites ranged from 3860 to 4175 m. The streams of lowest and highest elevations were streams 2 and 3, respectively. Rhithral streams encompassed the widest range of elevation between 3860 and 4050 m. Kryal streams were generally higher in elevation than both rhithral and intermediate streams. Finally, the intermediate stream was located in between the elevations of streams 1 and 2.

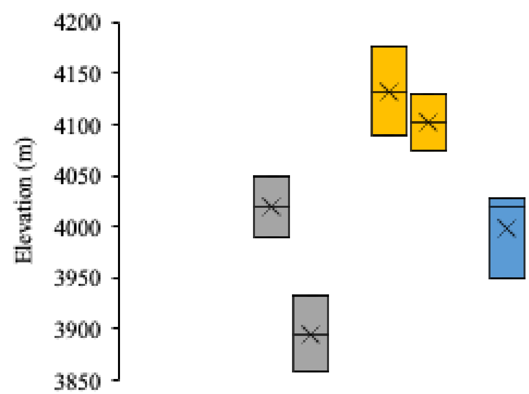

Figure 4.1. Elevation measurement range (m) for each stream. Gray bars signify rhithral streams 1 and 2, yellow bars signify kryal streams 3 and 4, and blue bars signify the intermediate stream 5.

Stream pH

As shown in Figure 5.1, pH of water at sites ranged from 6.6 to 8.43. Sites of lowest and highest pH were 5c and 2a, respectively. The intermediate stream exhibited the widest range of pH values between 6.6 and 8.1, while kryal streams exhibited the smallest range between 7.5 and 8.0. According to Figure 5.2, rates of stream pH change regarding elevation ranged from -0.00020 to -0.017 units/m, with streams 3 and 5 encompassing the smallest and largest values, respectively. Order of rate of pH change generally followed the trend of smallest rate of change in kryal streams, highest rate of change in intermediate streams, and intermediate rate of change in rhithral streams.

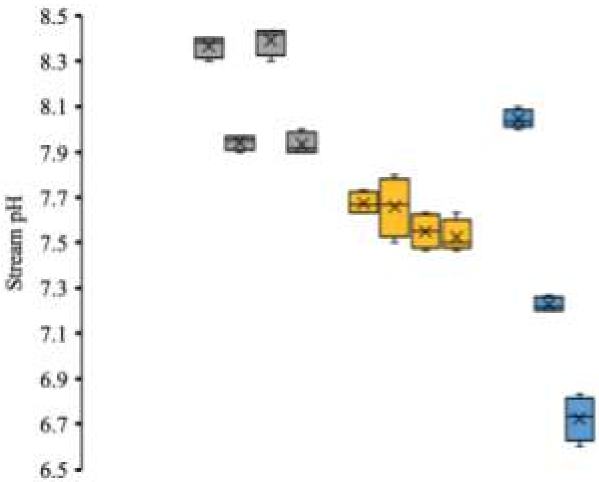

Figure 5.1. Stream pH for each site. Gray bars signify rhithral stream sites 1a, 1b, 2a, and 2b; yellow bars signify kryal stream sites 3a, 3b, 4a, and 4b; and blue bars signify intermediate sites 5a, 5b, and 5c.

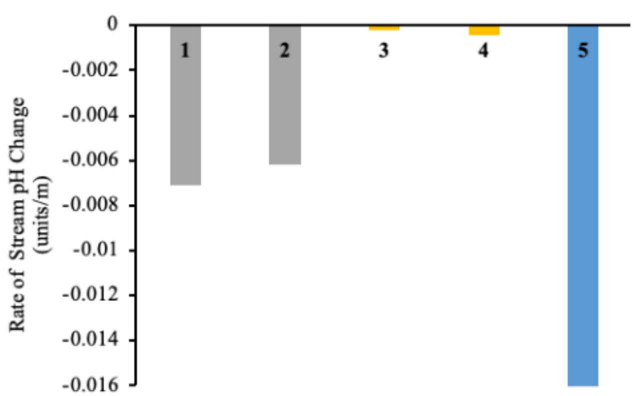

Figure 5.2. Rate of stream pH changes with respect to elevation (m) for all streams measured. Grey bars signify rhithral streams 1 and 2, yellow bars signify kryal streams 3 and 4, and blue bars signify the intermediate stream 5.

Stream Water Temperature

As shown in Figure 6.1, temperature of water at sites ranged from 5.6 to 15 ˚C, with sites 3b and 4a encompassing the lowest and highest temperature values, respectively. Kryal streams encompassed the widest range of temperature values, and the temperature values of both rhithral and intermediate streams fell within this range. As depicted in Figure 6.2, rates of stream water temperature change regarding elevation ranged from -0.032 to 0.015 °C/m, with streams 2 and 4 exhibiting the most positive and most negative values, respectively. Kryal and intermediate streams generally exhibited the highest rates of temperature change.

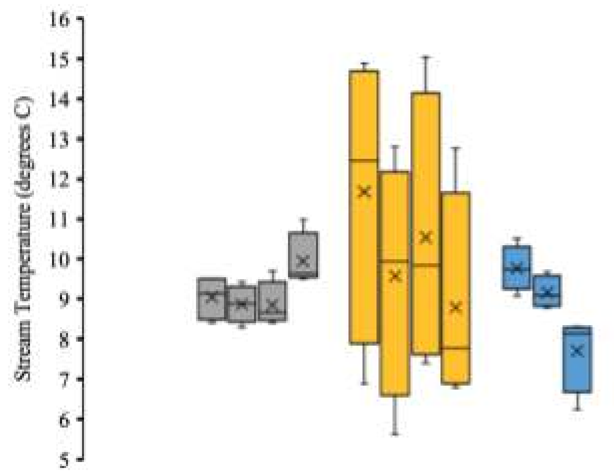

Figure 6.1. Stream water temperature (˚C) for each site. Gray bars signify rhithral stream sites 1a, 1b, 2a, and 2b; yellow bars signify kryal stream sites 3a, 3b, 4a, and 4b; and blue bars signify intermediate sites 5a, 5b, and 5c.

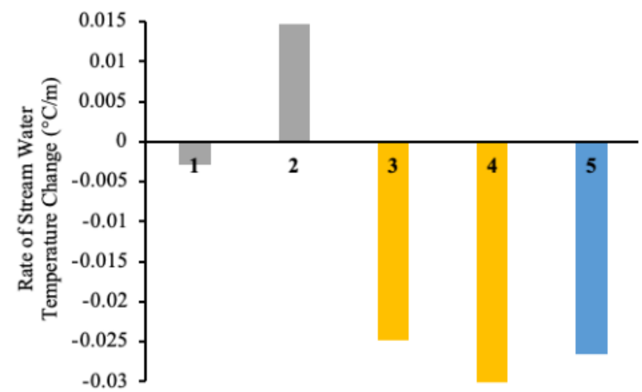

Figure 6.2. Rate of stream water temperature change with respect to elevation (˚C/m) for all streams measured. Grey bars signify rhithral streams 1 and 2, yellow bars signify kryal streams 3 and 4, and blue bars signify the intermediate stream 5.

Stream Discharge

As shown in Figure 7.1, stream discharge at sites ranged from 0.00029 to 0.37 m^3/s, with sites 2b and 5a encompassing the lowest and highest values, respectively. The intermediate stream exhibited generally higher discharge than other streams, followed by kryal streams and finally rhithral streams. According to Figure 7.2, rates of stream discharge change regarding elevation ranged from -0.0015 to 0.00072 $m^3s^{-1}m^{-1}$, with streams 4 and 5 exhibiting the most positive and most negative values, respectively. Order of rate of stream discharge change generally followed the trend of smallest rate of change in rhithral streams, highest rate of change in intermediate streams, and intermediate rate of change in kryal streams.

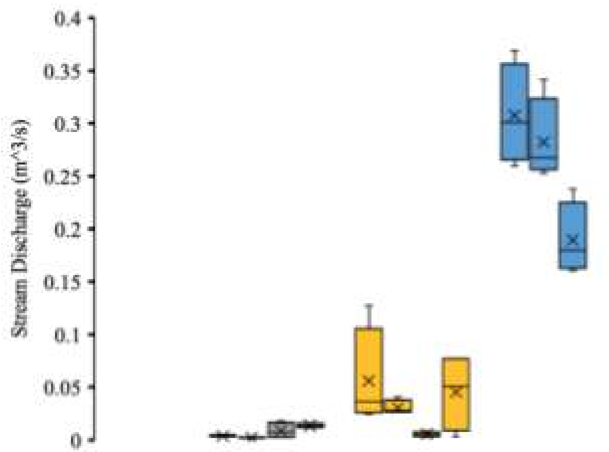

Figure 7.1. Stream discharge (m^3/s) for each site. Gray bars signify rhithral stream sites 1a, 1b, 2a, and 2b; yellow bars signify kryal stream sites 3a, 3b, 4a, and 4b; and blue bars signify intermediate sites 5a, 5b, and 5c.

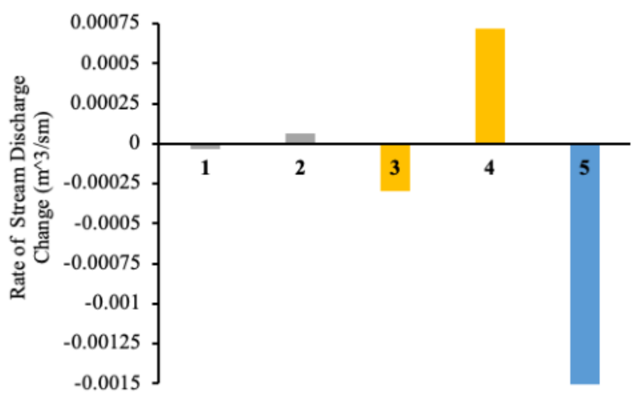

Figure 7.2. Rate of stream discharge changes with respect to elevation (m^3s^{-1}/m) for all streams measured. Grey bars signify rhithral streams 1 and 2, yellow bars signify kryal streams 3 and 4, and blue bars signify the intermediate stream 5.

Stream Turbidity

As shown in Figure 8.1, stream turbidity at sites ranged from 0 to 5, with multiple sites encompassing this lowest value and site 3a encompassing the highest. Kryal streams generally exhibited higher turbidity values than other sites.

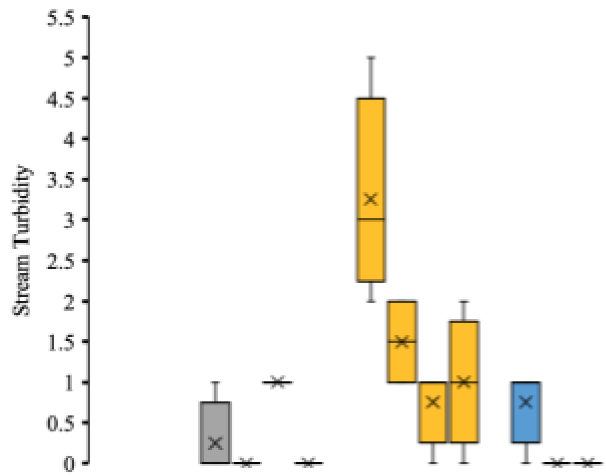

Figure 8.1. Stream turbidity for each site. Gray bars signify rhithral stream sites 1a, 1b, 2a, and 2b; yellow bars signify kryal stream sites 3a, 3b, 4a, and 4b; and blue bars signify intermediate sites 5a, 5b, and 5c.

Principal Component Analysis

Figures 9.1-9.3 depict principal component analyses (PCA) for stream variables within rhithral, kryal, and intermediate streams.

As shown in Figure 9.1, rhithral stream 1 showed a high degree of correlation between pH and stream discharge, with these variables both being negatively correlated with altitude. Water temperature and turbidity were negatively correlated with each other, and were not correlated with other variables. Rhithral stream 2 saw a high degree of correlation between pH and turbidity, with both of these variables strongly negatively correlated with altitude. Stream discharge and water temperature were slightly positively correlated, although these variables were not correlated with the others.

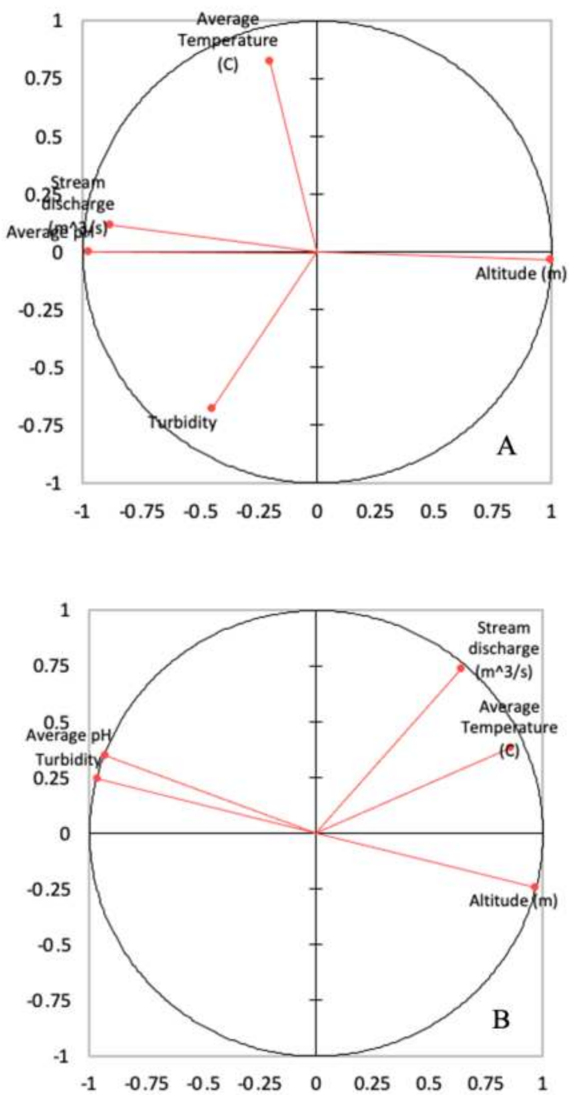

Figure 9.1. PCA of stream characteristics for (A) rhithral stream 1 and (B) rhithral stream 2.

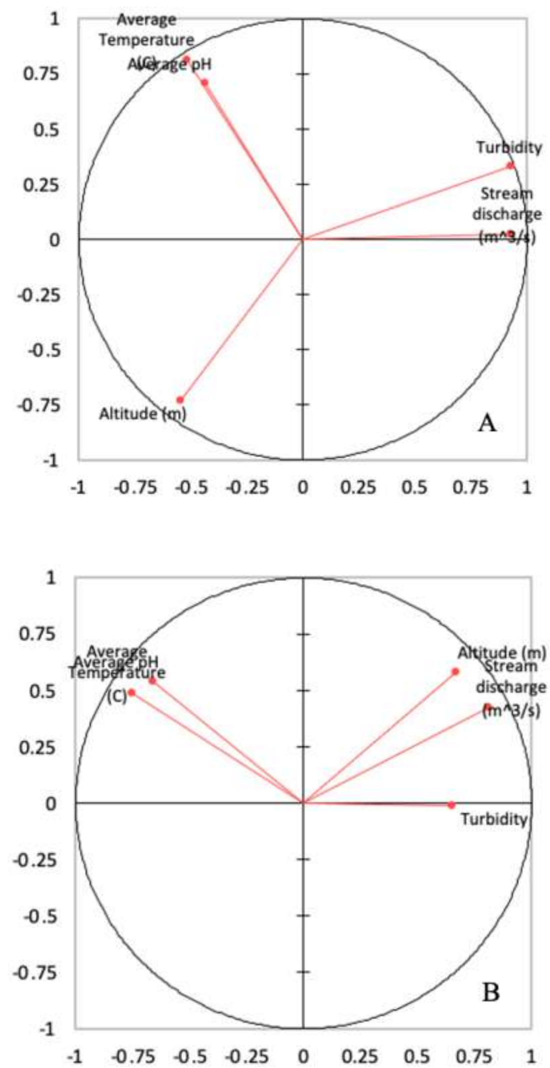

Figure 9.2. PCA of stream characteristics for (A) kryal stream 3 and (B) kryal stream 4.

Figure 9.2 depicts kryal streams with very similar correlations. There were very high degrees of positive correlation between water temperature and pH, as well as strong positive correlations between stream discharge and turbidity. In stream 3, altitude was generally negatively correlated with turbidity and stream discharge and not correlated with stream water temperature and pH. In stream 4, altitude was again not correlated with water temperature and pH, but strongly positively correlated with stream discharge and turbidity.

As shown in Figure 9.3, stream discharge and water temperature in the intermediate stream were strongly positively correlated. These two variables were roughly positively correlated with pH and turbidity, although to a lesser degree. Altitude was very negatively correlated with pH and turbidity, and to a lesser degree stream discharge and water temperature.

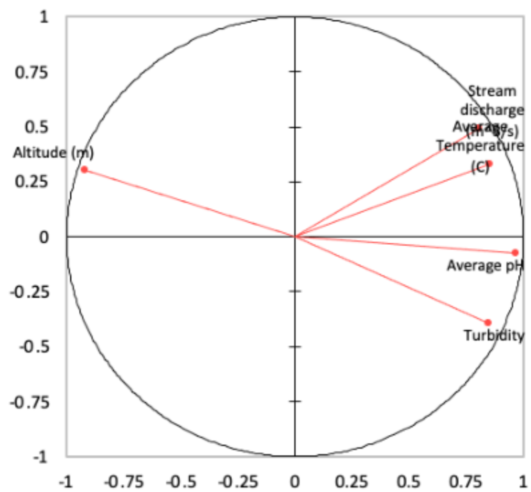

Figure 9.3. PCA of stream characteristics for the intermediate stream 5.

Stream Parameters

As depicted in Figure 10.1, stream width ranged from 0.15 to 2.8 m, while stream depth ranged from 0.012 to 0.26 m. Generally, for every 0.1 m of increase in stream depth, stream width increased 1 m. However, above 0.1 m of stream depth, stream width seemed to jump to around 2.5 m. Nearing 0.2 m of stream depth, stream width again fell to 1 meter and remained constant thereafter.

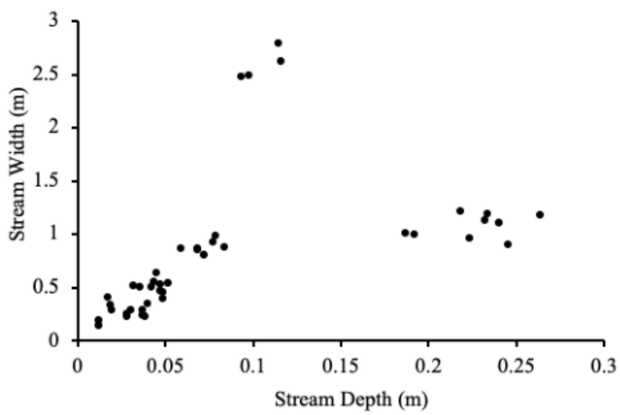

Figure 10.1. Average stream depth (m) plotted against average stream width (m) for all sites.

Climate Data

As shown in Figure 11.1, total daily precipitation ranged from 0 to 26 mm, with the driest days falling in the final week of the study, and the wettest day on April 23rd. Average daily precipitation throughout the 3 weeks studied was 6.86 mm.

Average daily air temperature ranged from 5.3 to 7.4 ˚C, as depicted in Figure 11.2, with the coldest day falling on April 23rd and the warmest on May 4th and May 5th. Average daily air temperature throughout the 3 weeks studied was 6.91 ˚C.

As shown in figure 11.3, average daily relative humidity ranged from 78 to 91%, with the least and most humid days falling on May 2nd and April 20th, respectively. Average daily relative humidity throughout the 3 weeks studied was 84%.

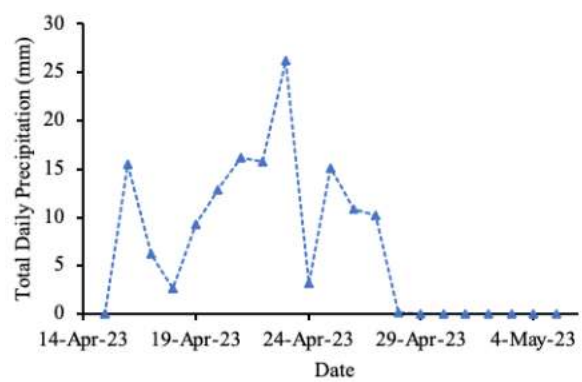

Figure 11.1. Total daily precipitation data (mm) between April 15th and May 5th, 2023.

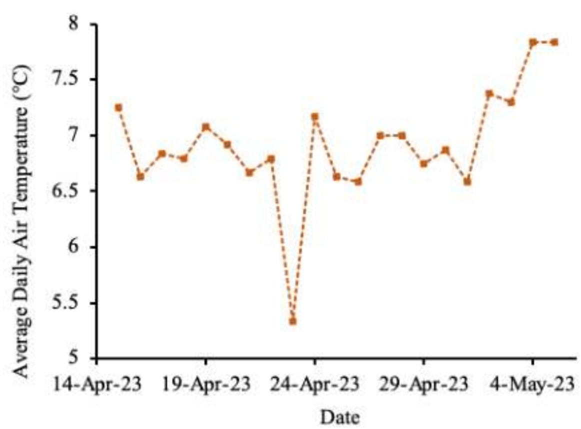

Figure 11.2. Average daily air temperature (˚C) data between April 15th and May 5th, 2023.

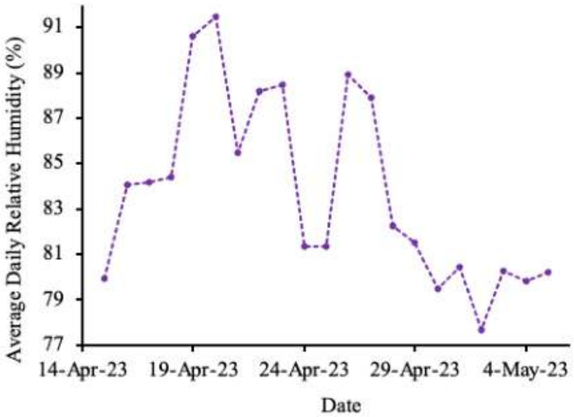

Figure 11.3. Average daily relative humidity (%) data between April 15th and May 5th, 2023.

As depicted in Figure 11.4, total daily precipitation and average daily air temperature appeared inversely correlated ($p = 0.34$), with roughly a 13 mm increase in precipitation between days corresponding with a decrease in air temperature of 1 ˚C.

Conversely, according to Figure 11.5, total daily precipitation and average daily relative humidity appeared generally directly correlated ($p < 0.001$), with a spike in relative humidity yielding an increase in precipitation approximately 3 days later.

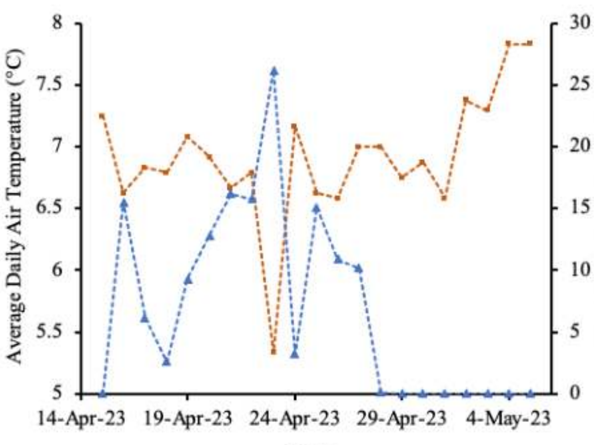

Figure 11.4. Total daily precipitation (mm) data against average daily air temperature (˚C) data between April 15th and May 5th, 2023. Precipitation is shown in blue triangles, while air temperature is shown in orange squares.

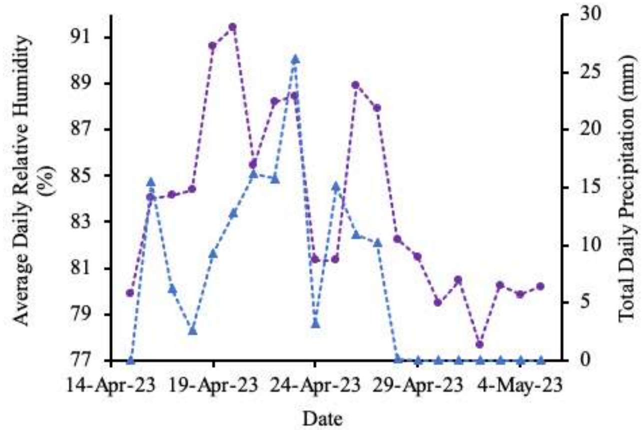

Figure 11.5. Total daily precipitation (mm) data against average daily relative humidity (%) data between April 15th and May 5th, 2023. Precipitation is shown with blue triangles, while relative humidity is shown in purple circles.

Climate & Stream Data

According to Figures 12.1 and 12.2, average stream water temperature for rhithral and intermediate streams during the 3 weeks studied followed the general trend of increasing 1.5 ˚C before decreasing. Water temperature in kryal streams increased by roughly 7 ˚C during the study, only beginning to decrease again in the final stream measurements. Intermediate streams generally followed the trend of rhithral streams.

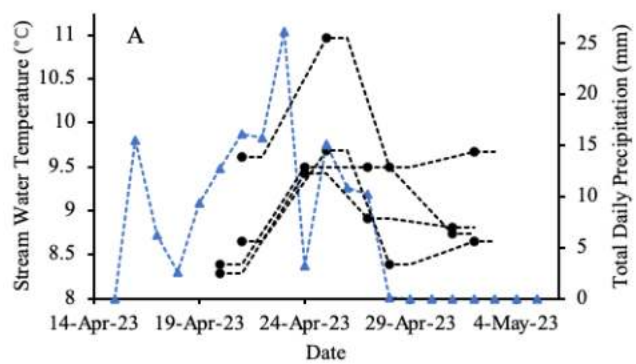

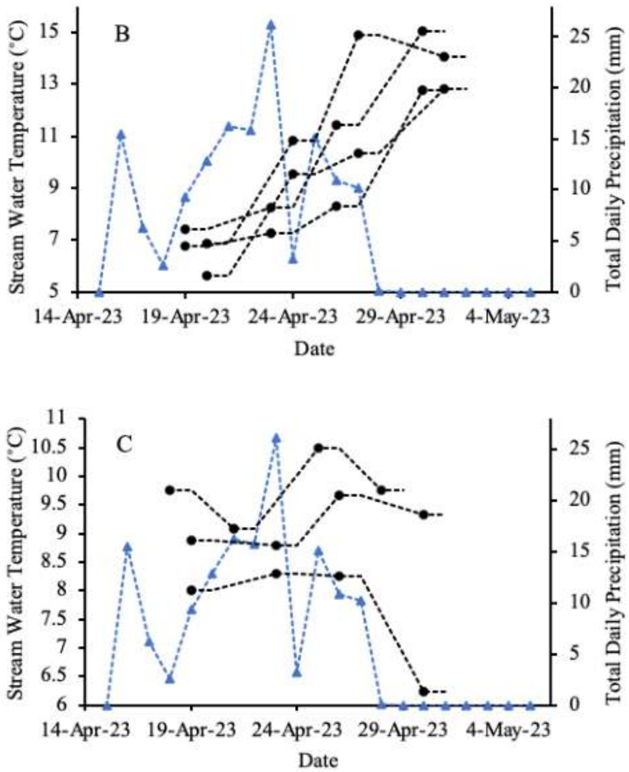

Figure 12.1. Total daily precipitation (blue triangle) and average water temperature (black circle) for (A) rhithral streams, (B) kryal streams, and (C) intermediate streams.

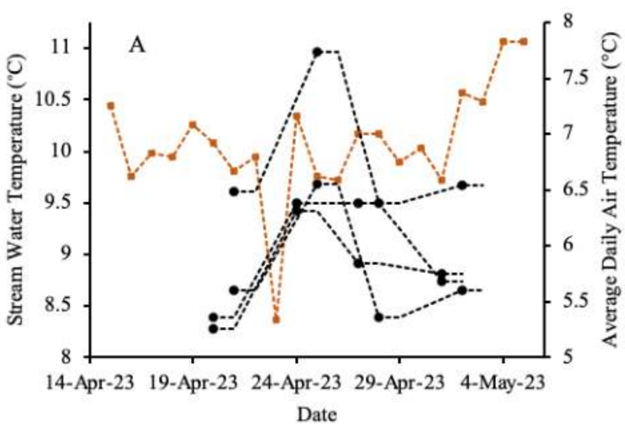

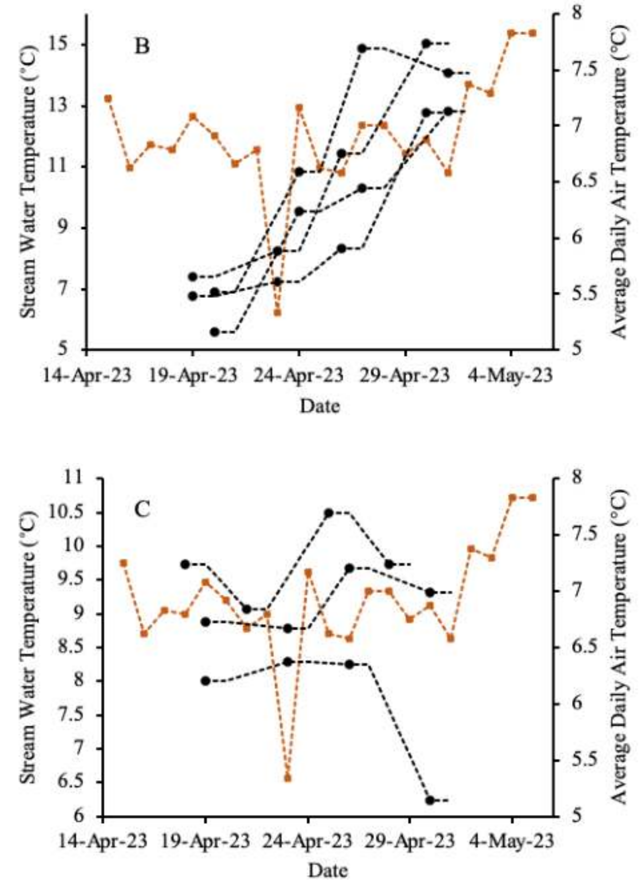

Figure 12.2. Average daily air temperature (orange square) and average water temperature (black circle) for (A) rhithral streams, (B) kryal streams, and (C) intermediate streams.

As can be seen in Figures 12.3 and 12.4, average stream discharge for kryal streams was variable, with sites 3a and 3b immediately decreasing followed by an increase, and others enduring a period of increase before decreasing. Discharge for rhithral streams consisted of a general trend of increase followed by a decrease, and a final increase toward the end of the study period. Stream 1a behaved differently, beginning in a decreasing trend. Intermediate streams generally followed the trend of a decrease in discharge throughout the study period.

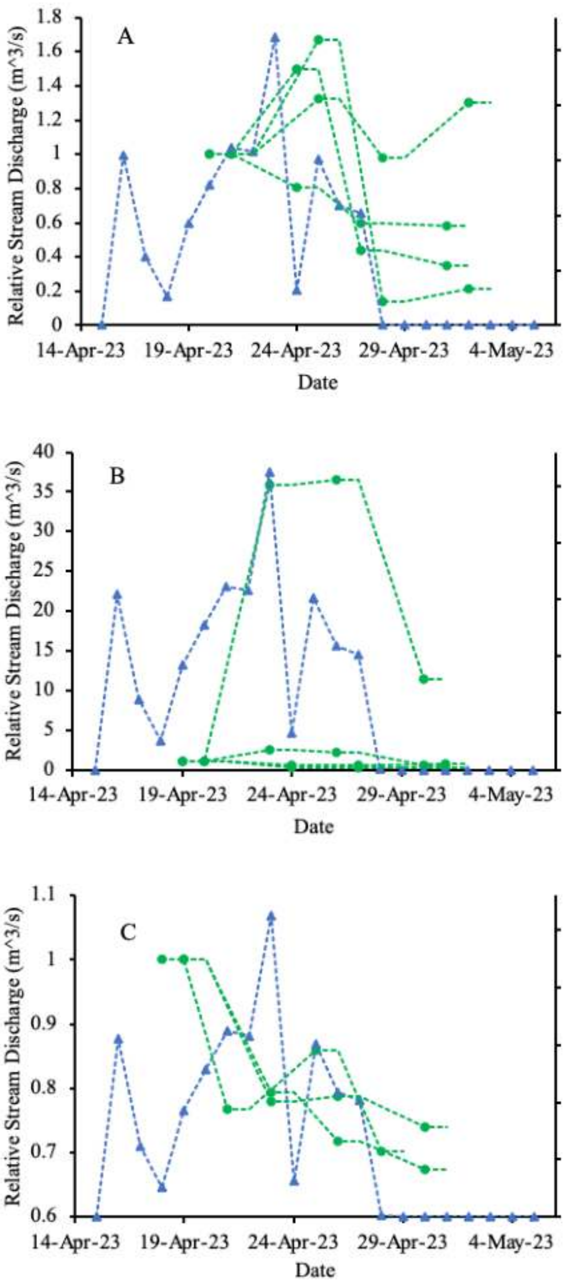

Figure 12.3. Total daily precipitation (blue triangle) and average stream discharge (green circle) for (A) rhithral streams, (B) kryal streams, and (C) intermediate streams.

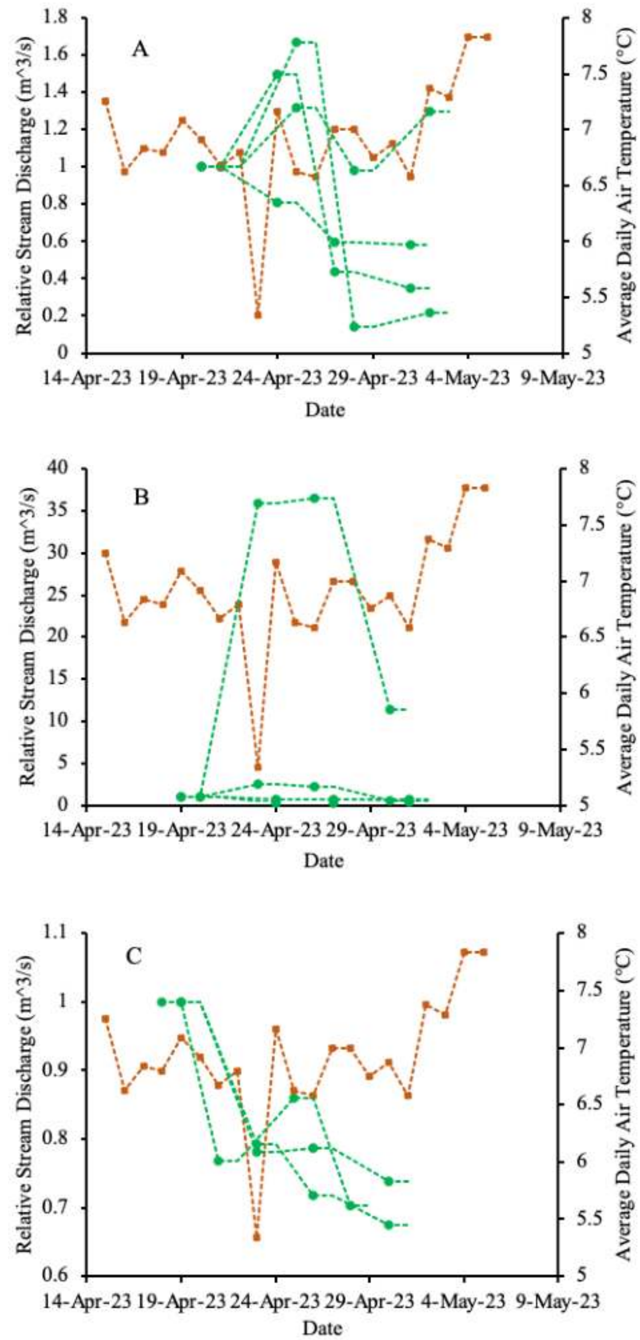

Figure 12.4. Average daily air temperature (orange square) and average stream discharge (green circle) for (A) rhithral streams, (B) kryal streams, and (C) intermediate streams.

As depicted in Table 1, the effect of total daily precipitation on average stream water temperature in rhithral and kryal streams was non-significant excluding stream sites 2b and 3a. Within kryal streams, precipitation had a generally less significant effect on sites 3b and 4b when compared to their lower elevation counterparts. In intermediate streams, the effect of precipitation on stream temperature was also non-significant and became less significant from sites 5a to 5c.

The effect of average daily air temperature on average stream water temperature was significant in all rhithral streams. In kryal streams, the effect of air temperature on stream water temperature was almost significant excluding site 3a, which was significant. Intermediate stream water temperature was significantly affected by air temperature, with site 5c being slightly less significantly affected than sites 5a and 5b.

Finally, the effects of total daily precipitation and average daily air temperature on stream discharge were significant for all sites.

It is important to note that statistical significance tests between average daily relative humidity and stream temperature and discharge were not conducted, as average daily relative humidity was strongly correlated with total daily precipitation, potentially yielding redundant results. Additionally, it is important to note that PCA analyses were not able to be conducted for climate and stream characteristic data because of the gaps in data between stream characteristic measurements.

Table 1. p-values for t-tests between stream parameters outlined above separated into rhithral (1a, 1b, 2a, 2b), kryal (3a, 3b, 4a, 4b), and intermediate streams (5a, 5b, 5c) with significant values bolded.

Site	P & WT[a]	P & SD[b]	AT & WT[c]	AT & SD[d]
1a	0.11	**< 0.001**	**< 0.001**	**< 0.001**
1b	0.13	**< 0.001**	**< 0.001**	**< 0.001**
2a	0.13	**< 0.001**	**< 0.001**	**< 0.001**
2b	**0.045**	**< 0.001**	**< 0.001**	**< 0.001**
3a	**0.042**	**< 0.001**	**0.030**	**< 0.001**
3b	0.13	**< 0.001**	**0.047**	**< 0.001**
4a	0.081	**< 0.001**	**0.047**	**< 0.001**
4b	0.20	**< 0.001**	0.073	**< 0.001**
5a	0.053	**< 0.001**	**< 0.001**	**< 0.001**
5b	0.097	**< 0.001**	**< 0.001**	**< 0.001**
5c	0.32	**< 0.001**	0.11	**< 0.001**

Statistical significance test of [a] total daily precipitation and stream water temperature, [b] total daily precipitation and stream discharge, [c] average daily air temperature and stream water temperature, [d] average daily air temperature and stream discharge.

ANALYSIS & DISCUSSION

Using the aforementioned data and observations made during the period of data collection, the conclusion may be drawn that the glaciers on the southwestern aspect of the Chimborazo volcano are nearing the end of their lives and have already passed the threshold in which they may predominantly have influence over streamflow.

Several trends in analyzed data pointed to this conclusion. First, the trend observed in Chimborazo glacier recession was very negative, most likely due to not only warming air temperatures in the region but also the exacerbation of this warming at higher altitude (Sklenář et al., 2021). Between 1965 and 2019, Chimborazo glaciers lost 42.5% of their surface area. This corresponds with a glacial surface area decline of 0.16 km^2 per year in that period. Additionally, using the created trendline, 50% loss of glacial coverage on the volcano relative to its coverage in 1965 is expected by the year 2026 (**Figure 3.1**). However, this trend corresponds to only the overall glacier surface area of the mountain and does not consider variations in weather due to Chimborazo's rain shadow.

On the southwestern aspect of the mountain where data was collected, temperatures are warmer and rainfall is minimal (Sklenář and Lægaard, 2003). These factors have further exacerbated glacier recession, as warmer temperatures have more quickly melted ice, and a lack of rainfall has prevented its buildup during the wet season. On current satellite images, glaciers on the southwestern aspect of the volcano descend to only 6,000 m. Since 1969, this corresponds to a 20% increase in glacial elevation from sea level. This, in accordance with the fact that the mountain itself extends only 300 m higher than this elevation, is evidence that the degree of glacial recession on the southwestern aspect of Chimborazo is most likely much larger than the 42.5% calculated for that of its glaciers overall.

Second, analyses of stream characteristics like pH, water temperature, discharge, and turbidity that were studied as an indirect measure of current glacial health largely supported a decreasing influence of glacial melt on kryal streams.

First, kryal streams contained the warmest temperatures of all stream types by almost 4 ˚C, with their coldest temperatures reaching only 5.5 ˚C (**Figure 6.1**). This was not expected, as kryal streams are known to not exceed 4 ˚C and exhibit little variation in water temperature due to regulation from glacial melt (Ward, 1994). This result corroborated glacial recession data, showing that a lack of glaciers on this aspect of the mountain no longer allow kryal streams to have their distinct characteristics.

Additionally, the intermediate stream began at a very low temperature at site 5c (**Figure 6.1**). This is an interesting result, as groundwater temperature is generally equal to the mean air temperature above ground and rarely fluctuates throughout the year (Kaandorp et al., 2019). This, corroborated with the current presence of the wet season in Ecuador and subsequently colder air temperature, should signify a generally warmer water temperature at site 5c. However, this is not the case. This may be due to the degree to which climate change has caused air temperature in the Chimborazo Reserve to increase. Groundwater temperature, which already rarely fluctuates, is not able to increase at this rate, and therefore remains cold compared to other water bodies in the region. This trend proves a degree of temperature increase in the region that may explain the extent to which glacial melt is occurring.

Kryal streams had generally larger discharge than rhithral streams (**Figure 7.1**), as they encompass a larger drainage basin, collecting water from large parts of the southwestern aspect of Chimborazo. However, there was generally a greater degree of variation in kryal streams than expected, indicating that a factor other than glacial melt may be regulating their discharge. Normally, a larger degree of glacial melt would be expected during drier periods and a lesser one during wetter periods (Huss and Hock, 2018; Marazi and Romshoo, 2018). Thus, the higher than expected variation in stream discharge observed in kryal streams indicates a significant loss of glacial influence.

Turbidity was highest in kryal streams (**Figure 8.1**), contrary to what was expected. Due to a lack of vegetation on the slopes of the Chimborazo volcano that hold soil together, sediment is looser (Gyssels et al., 2005). Even so, with a healthy degree of glacial influence on streamflow, this constant flow volume would not pick up a large amount of sediment. However, as glacial influence decreases and streamflow becomes more variable, kryal streams may pick up more sediment and become more turbid. This result was corroborated by PCA analyses of kryal streams, as stream discharge and turbidity were seen to have high degrees of positive correlation (**Figure 9.2**) that were absent from those of rhithral stream sites. Thus, both the higher level and range of turbidity in kryal streams signifies decreased glacial influence. Additionally, after a period of intense rainfall, turbidity was observed to be its highest in kryal streams, an unexpected result unless streamflow is primarily affected by climate, which again would indicate reduced glacial influence, as true kryal streams are predominantly influenced by glacial melt (Stahl et al., 2008; Williamson et al., 2019).

In addition to stream characteristic measurements indicating glacial recession, the correlational relationship between climate data and stream water temperature and discharge further proved this result. First, for all stream sites, precipitation and air temperature were significantly correlated with stream discharge (**Table 1**). The importance of these results lies in how stream temperatures and discharges changed throughout the 3-week study period. All rhithral stream sites saw an increase in stream discharge with an increase in precipitation and decrease in temperature (**Figures 12.3 & 12.4**). This was to be expected, as they are fed by rainwater, and thus will increase in discharge with a higher degree of precipitation. Within kryal stream sites, however, 4a and 4b saw increases in stream discharge by 40 times, while 3a and 3b decreased in discharge (**Figures 12.3 & 12.4**). This result was unexpected, as all kryal streams should theoretically experience decreases in stream discharge within these climatic conditions (Huss and Hock, 2018; Marazi and Romshoo, 2018). When precipitation increases and a corresponding drop in air temperature is observed, snow and ice begin to refreeze and be replenished by new precipitation, yielding a decrease in stream discharge (Pabón-Caicedo et al., 2020; Vuille, 2013). According to this data, stream 3 behaved like a kryal stream, while stream 4 did not.

Thus, the conclusion may be drawn that stream 4 is no longer a kryal stream, but a rhithral one instead. This makes sense, as its source is located deeper in the mountain's rain shadow, and the degree of glacial recession is thus much higher. Additionally, although stream 3 responded as expected to weather changes, it is still too warm. This stream may thus still be considered kryal, however now nearing the threshold past which it will no longer be considered such.

Additionally, average daily air temperature and water temperature were significantly correlated for three of four kryal stream sites, albeit less so than for rhithral sites (**Table 1**). This made sense, as there is both a greater mass of water to warm and a greater degree of temperature control due to ice and snow melt in kryal streams (Huss and Hock, 2018; Marazi and Romshoo, 2018). However, the fact that the water temperature in these streams was still significantly affected by air temperature may point to the conclusion that the temperature controlling effects of glaciers is diminishing. Thus, these once kryal streams will now be expected to respond more drastically to changes in climate and weather patterns due to anthropogenic activity than they would have before glacial influence was greatly reduced.

To examine how these data have changed over time, they may be compared to those taken in the study of Tanner Thomas in the spring of 2022. This study was conducted at the same time of year and thus serves as a valid comparison. In this study, generally higher pH levels were found compared to those of Thomas' study (Thomas, unpublished, 2022). This might be explained through the increasing of the vegetation line in the area due to increasing air temperatures (Sklenář et al., 2021), allowing for an increase in the altitude of farmland. In a study conducted by Irshad et al. in 2013, the pH of livestock manure was found to be roughly 8.4 when fresh, raising the pH of stream water when in close proximity to it. Thus, as farmland increases in altitude, general stream pH in all areas of the reserve will see a correlated increase in pH. This result further corroborates a high rate of glacial recession, as quickly warming air temperatures bring about glacial melt.

This study also saw a lesser amount of stream discharge at rhithral sites, but a greater amount at kryal sites than those of Thomas' study (Thomas, unpublished, 2022). This change may corroborate the decrease in precipitation in the area that locals have experienced, albeit against the conclusions of the scientific literature (La Frenierre and Mark, 2017). Rhithral streams, which are fed by rainwater, have been decreasing in discharge, while kryal stream discharge has slightly increased due to increased snowmelt. This result also further exemplified glacial melt, as increases in snowmelt signify quickly receding glaciers.

Beyond correlations between climate and stream characteristics data, observations were made during data collection that support glacial recession. At lower elevation sites on kryal streams, large fluvial plains and gorges were observed (see Appendix B). These geomorphological features can be interpreted in two ways, both of which support the conclusion that glacial influence has severely decreased. First, they may imply that streambeds of kryal streams once supported a much higher degree of streamflow while the glacier was melting at rapid rates. However, after the 'peak water' threshold was passed, the streams shrunk dramatically, leaving behind large fluvial plains and ravines void of vegetation. Conversely, a study conducted by La Frenierre and Mark in 2017 found that as glaciers recede and the constancy of meltwater changes, kryal streams become much more susceptible to flash-flooding. Sites 3a, 3b, and 4a all exhibited a great deal of flash-flooding evidence, such as a lack of vegetation surrounding the stream, very loose soil, and larger stream basins than would be necessary given the volume of water present at each site. This may imply an increasing frequency of flash flooding at these kryal sites, and thus decreased influence of glaciers in stream regulation.

Finally, the conclusions drawn in this study seem to corroborate patterns seen in high altitude mountains throughout the Ecuadorian Andes. A study conducted by Jacobsen et al. in 2009 found no classical kryal zone on the western aspect of the Antisana volcano, with minimum temperatures of 8 ˚C in supposedly kryal streams. This not only suggests that the data in this study can be extrapolated to other areas of the Ecuadorian Andes, but also that the state of glaciers on the leeward aspects of these volcanoes has been in significant decline for some time. If this trend continues, many communities that depend on Chimborazo and other large mountains for their water will have to find new water sources, and many downstream ecosystems that depend on these glaciers will suffer.

While data largely supported glacial recession, there were some data that supported the opposite. First, kryal streams predictably exhibited a greater degree of water temperature increase with respect to altitude than other stream types (**Figure 6.2**). This is most likely due to the lack of plant cover on these streams as a result of higher altitude. This exposed stream surface lacks protection from the sun and can thus warm more quickly (Trimmel et al., 2018).This result did not dictate glacial recession, but rather an established characteristic of kryal streams.

Additionally, the pH ranges of kryal streams were consistent with predicted results as they were generally lower than those of rhithral streams (**Figure 5.1**), and there was a smaller degree of pH change with respect to elevation (**Figure 5.2**). Since kryal streams are sourced at higher elevation, and therefore on steeper slopes and in colder air temperatures, the presence of farmland near these streams is limited. Given that the deposition of organic waste by farm animals has the potential to raise stream pH (Irshad et al., 2013), the lack of nearby farmland limited the degree to which kryal stream pH could be raised. In this case, kryal streams seem to behave appropriately, albeit at a higher base pH level than in previous years (Thomas, unpublished, 2022). These results indicated that cooler air temperatures exist at higher elevation on the mountain, and therefore most likely greater amounts of ice and snow.

With respect to climate data, total daily precipitation and water temperature changes were not significantly correlated for rhithral or kyral streams (**Table 1**). Since rhithral streams are mostly fed by rainwater, an increase in rainfall would not affect their temperature to a significant degree. Conversely, average daily air temperature and water temperature were significantly correlated for all rhithral stream sites (**Table 1**). This makes sense, as given less stream discharge in rhithral streams, an increase in air temperature would more effectively warm their smaller mass of water. For kryal streams, the correlations between total daily precipitation and water temperature values were almost statistically significant (**Table 1**). This may be because the higher temperature of rainfall should have the potential to more greatly influence kryal streamwater that is fed by snow and glacial melt. However, the fact that this correlation is still not significant may suggest a degree of temperature regulation by snowmelt. This result thus indicated that kryal streams on this aspect of the mountain are still behaving as expected.

Although great care was taken to ensure accuracy and precision in data collection, there were several sources of error that may have affected conclusions. The first could be inaccuracy in measuring methods, specifically relating to stream velocity in low-discharge streams. There may have been inaccuracy in distance measurement because of stream contours, as well as error in the time denoted for an object to reach the end of the tape measure of a given distance. This may have created error in calculations for stream discharge.

A second source of error may have been human activity on streams, specifically in stream site 2a. The Concreto Chimborazo company's presence on this stream caused it to have questionable results relating to temperature and discharge, and for this reason it was largely ignored in data analysis. Confounding data from this stream site manifested itself in several ways.

First, rhithral streams exhibited a lesser degree of temperature change with respect to altitude, as they were generally surrounded by more vegetation. Stream 2 was a unique case, with an increase in altitude corresponding with an increase in water temperature (**Figure 6.2**). This result was possibly affected by variability due to a decreased volume of water flow.

Additionally, similarly to Thomas' study, this study found generally higher turbidity in kryal streams. However, in Thomas' study, site 2a also saw a large amount of turbidity, a detail absent from this study (Thomas, unpublished, 2022). Piecing this together with a larger discharge at site 2a compared to 2b, Thomas must have taken these measurements when water from stream 2 was not being channeled by the Concreto Chimborazo company upstream of site 2a. This influx of water at 2a would have picked up sediment, giving Thomas his higher turbidity measurement at that site.

Moreover, it is generally accepted that stream discharge and elevation are negatively correlated, yet streams 2 and 4 provided evidence to the contrary (**Figure 7.2**). In stream 2, this peculiarity can again be credited to site 2a lying below a rechanneling canal owned by the Concreto Chimborazo company. With enough of this water removed from the stream, site 2a may be left with less discharge than its upstream counterpart.

In stream 4, however, the irregularity of this pattern may be due to a natural cause. The soil around site 4a is extremely loose, making it very permeable to water (see Appendix B). During the process of data collection, the water of stream 4 was observed to be disappearing into this loose soil downstream of site 4a. Thus, as the water from site 4b travels downstream, much of it may be seeping into this loose soil, yielding a comparatively lower stream discharge at site 4a.

In PCA analyses, this error was visualized in the altitude of streams 2 and 4 sites not being strongly negatively correlated with stream discharge (**Figures 9.1 & 9.2**), as is generally expected for any stream, as they gain greater volumes of water as they lose elevation.

Finally, a source of error of all data in this study could be that the examination of precipitation with respect to stream flow was conducted over a relatively short 3-week period. Most studies that examined precipitation with respect to stream flow were conducted over long periods of time (Gordillo and Pineda, 2021; Pellicciotti et al., 2007). This short period may thus not include patterns observed in other longer studies.

Future studies on this subject may seek to explore the ways in which glacier recession and climate affect streamflow on the northeastern aspect of the volcano, as temperatures are cooler, there is more cloud cover, and rainfall replenishes melting ice during the wet season (Sklenář and Lægaard, 2003). The glaciers there have not receded as much as on the southwestern aspect, and it may be interesting to determine whether they have also reached their 'peak water' threshold or are in the process of doing so. Other studies may also explore streamflow and quality at higher elevations than the 4175 m reached in this study, as proximity to glacier coverage may influence streamflow to a greater extent. Finally, future research may examine the effects of the channeling of water by the Concreto Chimborazo company in different parts of the Reserve on aquatic biodiversity.

NOTES

The author would like to note no conflict of interest in the research presented in this study.

AUTHOR INFORMATION

Phone: +1 (425) 785-7691.

Email: wfpa2020@mymail.pomona.edu.

Address: 13708 NE 32nd Pl Bellevue, Washington 98005.

REFERENCES

Aguilar-Lome, J., Espinoza-Villar, R., Espinoza, J.-C., Rojas-Acuña, J., Willems, B. L., & Leyva-Molina, W.-M. (2019). Elevation-dependent warming of land surface temperatures in the Andes assessed using MODIS LST time series (2000–2017). *International Journal of Applied Earth Observation and Geoinformation*, *77*, 119–128. https://doi.org/10.1016/j.jag.2018.12.013

Alvarez-Mendoza, C. I., & Ramirez-Cando, L. (2022). Simplified analysis of the influence of climate change on the melting of Chimborazo Mountain Glacier using partial least squares (PLS) and remote sensing. *Remote Sensing for Agriculture, Ecosystems, and Hydrology XXIV*. https://doi.org/10.1117/12.2634043

Bro, R., & Smilde, A. K. (2014). Principal component analysis. *Anal. Methods*, *6*(9), 2812–2831. https://doi.org/10.1039/c3ay41907j

Chang, M. (2019, May 11). *A Macroinvertebrate Water Quality Study in Chinchin Stream, Ecuador: Characterizing the Effects of Small Scale Deforestation and Agriculture on Freshwater Ecosystems*. https://docs.google.com/document/d/1SV_EX1gcfT6csIiSxC-wUcXr6GI-InqKTfaqQBjOBqA/edit

Chevallier, P., Pouyaud, B., Suarez, W., & Condom, T. (2010). Climate change threats to environment in the tropical andes: Glaciers and Water Resources. *Regional Environmental Change*, *11*(S1), 179–187. https://doi.org/10.1007/s10113-010-0177-6

Clapperton, C. M. (1990). Glacial and volcanic geomorphology of the Chimborazo-Carihuairazo Massif, Ecuadorian andes. *Earth and Environmental Transactions of the Royal Society of Edinburgh*, *81*(2), 91–116. https://doi.org/10.1017/s0263593300005174

Dyurgerov, M., & Meier, M. (2005). *Glaciers and the Changing Earth System: A 2004 Snapshot*.

Ely, C. P., & Martin, D. J. (2018). Investigating the geomorphic characteristics of an Amazonian headwater stream draining a páramo ecosystem. *Physical Geography*, *40*(2), 164–185. https://doi.org/10.1080/02723646.2018.1513289

Giles, M. P., Michelutti, N., Grooms, C., & Smol, J. P. (2018). Long-term limnological changes in the Ecuadorian páramo: Comparing the ecological responses to climate warming of shallow waterbodies versus Deep Lakes. *Freshwater Biology*, *63*(10), 1316–1325. https://doi.org/10.1111/fwb.13159

Gordillo, J., & Pineda, L. E. (2021). Unravelling runoff processes in Andean basins in northern Ecuador through hydrological signatures. *Hydrological*

Processes, *35*(9). https://doi.org/10.1002/hyp.14354
Gyssels, G., Poesen, J., Bochet, E., & Li, Y. (2005). Impact of plant roots on the resistance of soils to erosion by water: A Review. *Progress in Physical Geography: Earth and Environment*, *29*(2), 189–217. https://doi.org/10.1191/0309133305pp443ra
Huss, M., & Hock, R. (2018). Global-scale hydrological response to future glacier mass loss. *Nature Climate Change*, *8*(2), 135–140. https://doi.org/10.1038/s41558-017-0049-x
Irshad, M., Eneji, A. E., Hussain, Z., & Ashraf, M. (2013). Chemical characterization of fresh and composted livestock manures. *Journal of Soil Science and Plant Nutrition*, (ahead), 0–0. https://doi.org/10.4067/s0718-95162013005000011
Jacobsen, D., Dangles, O., Andino, P., Espinosa, R., Hamerlík, L., & Cadier, E. (2009). Longitudinal zonation of macroinvertebrates in an Ecuadorian glacier-fed stream: Do tropical glacial systems fit the temperate model? *Freshwater Biology*, *55*(6), 1234–1248. https://doi.org/10.1111/j.1365-2427.2009.02348.x
Kaandorp, V. P., Doornenbal, P. J., Kooi, H., Peter Broers, H., & de Louw, P. G. B. (2019). Temperature buffering by groundwater in ecologically valuable lowland streams under current and future climate conditions. *Journal of Hydrology X*, *3*, 100031. https://doi.org/10.1016/j.hydroa.2019.100031
La Frenierre, J., & Mark, B. G. (2017). Detecting patterns of climate change at Volcán Chimborazo, Ecuador, by integrating instrumental data, public observations, and Glacier Change Analysis. *Annals of the American Association of Geographers*, *107*(4), 979–997. https://doi.org/10.1080/24694452.2016.1270185
Marazi, A., & Romshoo, S. A. (2018). Streamflow response to shrinking glaciers under changing climate in the Lidder Valley, Kashmir Himalayas. *Journal of Mountain Science*, *15*(6), 1241–1253. https://doi.org/10.1007/s11629-017-4474-0
Miranda, L. (2019, May). *Petroleum Industry Impacts in the Ecuadorian Amazon: Water Quality and Perceptions of the Oil Industry in Loma del Tigre*. https://docs.google.com/document/d/1-MnzaRfNg1qsmbRe_zzTDHJn0fUUFlxs/edit
Mountain Research Initiative Edw Working Group, Pepin, N., Bradley, R. S., Diaz, H. F., Baraer, M., Caceres, E. B., Forsythe, N., Fowler, H., Greenwood, G., Hashmi, M. Z., Liu, X. D., Miller, J. R., Ning, L., Ohmura, A., Palazzi, E., Rangwala, I., Schöner, W., Severskiy, I., Shahgedanova, M., & Wang, M. B. (2015). Elevation-dependent warming in mountain regions of the world. *Nature Climate Change*, *5*(5), 424–430. https://doi.org/10.1038/nclimate2563
Pabón-Caicedo, J. D., Arias, P. A., Carril, A. F., Espinoza, J. C., Borrel, L. F., Goubanova, K., Lavado-Casimiro, W., Masiokas, M., Solman, S., & Villalba, R. (2020). Observed and projected hydroclimate changes in the Andes. *Frontiers in Earth Science*, *8*. https://doi.org/10.3389/feart.2020.00061
Padrón, R. S., Wilcox, B. P., Crespo, P., & Célleri, R. (2015). Rainfall in the Andean páramo: New insights from high-resolution monitoring in southern Ecuador. *Journal of Hydrometeorology*, *16*(3), 985–996. https://doi.org/10.1175/jhm-d-14-0135.1
Pellicciotti, F., Burlando, P., & van Vliet, K. (2007). Recent trends in precipitation and streamflow in the Aconcagua River Basin, central Chile. *IAHS Publications-Series of Proceedings and Reports*, *318*, 17–38.
Rabatel, A., Francou, B., Soruco, A., Gomez, J., Cáceres, B., Ceballos, J. L., Basantes, R., Vuille, M., Sicart, J.-E., Huggel, C., Scheel, M., Lejeune, Y., Arnaud, Y., Collet, M., Condom, T., Consoli, G., Favier, V., Jomelli, V., Galarraga, R., … Wagnon, P. (2013). Current state of glaciers in the tropical andes: A multi-century perspective on Glacier Evolution and Climate Change. *The Cryosphere*, *7*(1), 81–102. https://doi.org/10.5194/tc-7-81-2013
Ragettli, S., Immerzeel, W. W., & Pellicciotti, F. (2016). Contrasting climate change impact on river flows from high-altitude catchments in the Himalayan and Andes Mountains. *Proceedings of the National Academy of Sciences*, *113*(33), 9222–9227. https://doi.org/10.1073/pnas.1606526113
Rangwala, I., & Miller, J. R. (2012). Climate change in mountains: A review of elevation-dependent warming and its possible causes. *Climatic Change*, *114*(3–4), 527–547. https://doi.org/10.1007/s10584-012-0419-3
Sklenář, P., & Lægaard, S. (2003). Rain-shadow in the high Andes of Ecuador evidenced by Páramo vegetation. *Arctic, Antarctic, and Alpine Research*, *35*(1), 8–17. https://doi.org/10.1657/1523-0430(2003)035[0008:rsitha]2.0.co;2
Sklenář, P., Romoleroux, K., Muriel, P., Jaramillo, R., Bernardi, A., Diazgranados, M., & Moret, P. (2021). Distribution changes in páramo plants from the equatorial high Andes in response to increasing temperature and humidity variation since 1880. *Alpine Botany*, *131*(2), 201–212. https://doi.org/10.1007/s00035-021-00270-x
Stahl, K., Moore, R. D., Shea, J. M., Hutchinson, D., & Cannon, A. J. (2008). Coupled modelling of

Glacier and streamflow response to future climate scenarios. *Water Resources Research*, *44*(2). https://doi.org/10.1029/2007wr005956

Steffan, A. W. (1971). Chironomid (Diptera) BIOCOENOSES in Scandinavian glacier brooks. *The Canadian Entomologist*, *103*(3), 477–486. https://doi.org/10.4039/ent103477-3

Thomas, T. (2022, May). *Aquatic diversity in a changing tropical Andean glacierized catchment: Macroinvertebrates reveal possible important consequences to the Chimborazo region as glaciers recede and the climate continues to change* . https://docs.google.com/document/d/193whwuyIUyTF0xtguJ9ALn62HN1VEmn5B2x7O1MaY4M/edit

Trimmel, H., Weihs, P., Leidinger, D., Formayer, H., Kalny, G., & Melcher, A. (2018). Can riparian vegetation shade mitigate the expected rise in stream temperatures due to climate change during heat waves in a human-impacted pre-alpine river? *Hydrology and Earth System Sciences*, *22*(1), 437–461. https://doi.org/10.5194/hess-22-437-2018

Vuille, M. (2013). Climate Change and Water Resources in the Tropical Andes. *Inter-American Development Bank*.

Ward, J. V. (1994). Ecology of alpine streams. *Freshwater Biology*, *32*(2), 277–294. https://doi.org/10.1111/j.1365-2427.1994.tb01126.x

Williamson, R. J., Entwistle, N. S., & Collins, D. N. (2019). Meltwater temperature in streams draining alpine glaciers. *Science of The Total Environment*, *658*, 777–786. https://doi.org/10.1016/j.scitotenv.2018.12.215

APPENDIX A

Table 1. Data for stream parameters measured or calculated for all stream sites separated into rhithral (1a, 1b, 2a, 2b), kryal (3a, 3b, 4a, 4b), and intermediate streams (5a, 5b, 5c).

Site	Elevation (m)	pH	Temperature (˚C)	Depth (m)	Width (m)	Velocity (m/s)	Discharge (m^3/s)	Turbidity
1a	3990	8.3	8.39	0.038	0.237	0.380	0.0034	0
		8.4	9.50	0.037	0.250	0.301	0.0028	0
		8.4	9.50	0.028	0.250	0.288	0.0020	0
		8.4	8.74	0.028	0.253	0.278	0.0020	1
1b	4050	8.0	8.28	0.019	0.300	0.143	0.00083	0
		7.9	9.43	0.028	0.232	0.189	0.0012	0
		7.9	8.91	0.012	0.193	0.160	0.00036	0
		8.0	8.81	0.012	0.147	0.169	0.00029	0
2a	3858	8.4	8.65	0.047	0.530	0.400	0.0099	1
		8.4	9.69	0.045	0.643	0.571	0.017	1
		8.3	8.39	0.018	0.347	0.220	0.0014	1
		8.4	8.65	0.030	0.300	0.238	0.0021	1
2b	3932	7.9	9.61	0.048	0.407	0.536	0.011	0
		7.9	11.0	0.020	0.543	0.496	0.014	0
		7.9	9.50	0.032	0.527	0.619	0.010	0
		8.0	9.67	0.042	0.513	0.641	0.014	0
3a	4090	7.6	6.89	0.220	1.22	0.471	0.13	5
		7.6	11.0	0.072	0.813	0.488	0.028	3
		7.7	14.9	0.058	0.870	0.449	0.023	2
		7.7	14.0	0.077	0.930	0.573	0.041	3
3b	4175	7.5	5.61	0.078	0.990	0.504	0.039	2
		7.6	9.54	0.068	0.860	0.424	0.025	1
		7.8	10.3	0.068	0.877	0.413	0.025	1
		7.7	12.8	0.083	0.887	0.373	0.028	2
4a	4075	7.6	7.39	0.040	0.360	0.190	0.0027	1
		7.5	8.24	0.047	0.473	0.308	0.0068	1
		7.5	11.4	0.035	0.507	0.349	0.0062	0
		7.6	15.0	0.017	0.413	0.226	0.0016	1
4b	4130	7.5	6.78	0.037	0.293	0.194	0.0021	1
		7.5	7.24	0.048	0.467	3.31	0.075	1
		7.5	8.31	0.043	0.563	3.11	0.076	2
		7.6	12.8	0.025	0.337	2.82	0.024	0
5a	3950	8.0	9.74	0.233	1.20	1.31	0.37	1
		8.0	9.07	0.263	1.19	0.902	0.28	0
		8.1	10.5	0.240	1.11	1.19	0.32	1
		8.0	9.74	0.232	1.14	0.978	0.26	1
5b	4020	7.3	8.87	0.223	0.970	1.57	0.34	0
		7.2	8.78	0.245	0.910	1.19	0.27	0
		7.2	9.67	0.192	1.01	1.38	0.27	0
		7.2	9.31	0.187	1.01	1.33	0.25	0
5c	4028	6.6	8.00	0.114	2.80	0.739	0.24	0
		6.9	8.30	0.116	2.63	0.614	0.19	0
		6.8	8.26	0.098	2.50	0.695	0.17	0
		6.7	6.24	0.093	2.49	0.686	0.16	0

APPENDIX B

Figure 13.1. Rhithral data collection site 1a.

Figure 13.3. Rhithral data collection site 2a.

Figure 13.2. Rhithral data collection site 1b.

Figure 13.4. Rhithral data collection site 2b.

Figure 13.5. Kryal data collection site 3a.

Figure 13.6. Kryal data collection site 3b.

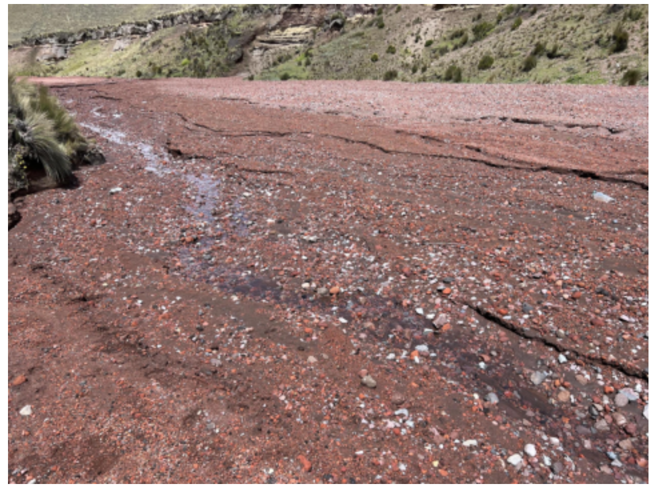

Figure 13.7. Kryal data collection site 4a.

Figure 13.8. Kryal data collection site 4b.

Figure 13.9. Intermediate data collection site 5a.

Figure 13.10. Intermediate data collection site 5b.

Figure 13.11. Intermediate data collection site 5c.